

Research Article

GEOLOGY

Burial and thermal history simulation of the Middle Jurassic source rocks in Matruh basin, north Western Desert, Egypt

Walaa A. Ali^{1*} and Mohamed Fagelnour²

^{1*} Petroleum Geology Department, Faculty of Petroleum and Mining Sciences, Matrouh University, Matrouh, 51511, Egypt

² Khalda Petroleum Company, Cairo, Egypt

Corresponding author: Walaa A. Ali

e-mail: Walaa.ali@mau.edu.eg

Received: 17/12/2023

Accepted: 1/1/2024

KEY WORDS

ABSTRACT

Matruh basin,
Khatatba
Formation
Jurassic source
rock,
1D basin
modeling,
Hydrocarbon
generation and
expulsion

The Middle Jurassic Khatatba Formation, a source rock for hydrocarbons in Egypt's Matruh basin, was modeled using geological and geochemical data from the Apidose-1X well. The 1D basin modeling helps construct burial and thermal geo-histories and predict petroleum and expulsion timings. Using the straightforward cracking method of Sweeny and Burnham (1990), PetroMod-1D software created the burial history model of the Apidos-1X well. The end of the Cretaceous to Early Tertiary to Late Paleocene (60–58 Ma ago) was characterized by a major uplifting phase due to tectonic inversion. The constructed models indicate that the Khatatba Formation entered the onset of oil generation in the Early Cretaceous period (115–116 Ma ago), while the onset of gas generation took place in the Oligocene period (22–24 Ma ago). Cracking of oil to gas was observed in the Middle Jurassic source rock in the Apidos-1X well. The Matruh Basin includes all the elements of the petroleum system, with shale source rocks from the Middle Jurassic, sandstone reservoir rocks from the Early and Middle Jurassic, and seal rock from the Early Cretaceous. Oil generation, migration, and accumulation began in the Early Cretaceous, with hydrocarbons charging traps during rifting phases. The basin modeling results suggest that the Middle Jurassic source rock acts as an effective source rock, where a significant amount of petroleum is expected to be generated and expelled to nearby prospect reservoir rocks in the Matruh basin.

Introduction

The Matruh Basin in Egypt's Western Desert contains numerous reservoirs that supply hydrocarbon-producing fields. The Matruh Basin has around 23 billion barrels of oil equivalent and 3 trillion cubic feet of gas deposits. According to EOG's report (2023), the Khatatba Formation reservoirs in the Matruh Basin have been producing about 64 million cubic feet of natural gas per day. The primary hydrocarbon source rocks in the Matruh Basin during the Mesozoic era include the Khatatba Formation from the Middle Jurassic period, the Alam El Bueib Formation from the the Early Cretaceous time, and the "G" Member of the Abu Roash Formations from the Upper Cretaceous time. These findings have been documented by various researchers, including **Meshref, (2000); Metwalli and Pigott, (2005); Shalaby et al., (2014)**. The studied area lies within the Matruh basin, which is part of the Khalda concession, in the northern Western Desert of Egypt. The origin generated hydrocarbons in Matruh Basin need to be studied in detail, in order to confirm its suitability for further petroleum exploration and development. The data set used herein is from the

Apidos-1X well in the Matruh Basin, which lies between latitude $30^{\circ} 55' 26.179''$ N and longitude $27^{\circ} 26' 27.081''$ E' as shown in Fig. (1). The main objective of this study of this study is to construct the burial and thermal maturity models of the studied Middle Jurassic Khatatba Formation source rocks in the Matruh Basin, north Western Desert simulate the timing of petroleum generation and expulsion, and evaluate the level of thermal maturity for these rocks in the Apidos-1X well within the Matruh Basin. This work was carried out using 1D PetroMod basin modeling.

Geologic Setting

The Matruh Basin is extending in the northeast and southwest directions of trending grabens. It formed during the Late Jurassic to Early Cretaceous period and is a part of the Unstable Shelf. The location is situated approximately within the coordinates of 26° and $27^{\circ} 30'$ E longitude and 31° and $31^{\circ} 17'$ N latitude (Fig. 1). The geological development of the basin is related to the tectonic processes that influenced the northern region of Egypt in the Mesozoic era (**Dolson et al., 2001; Moustafa, 2008, 2020**).



Fig. (1): Location map of the Matruh Basin along with other Mesozoic basins in the North Western Desert of Egypt and location of the studied Apidode-1X well (Modified after **EGPC, 1992, Mansour et al., 2023**).

The subsidence of the Matruh Basin initiated in the Paleozoic era and had renewed activity during the middle Mesozoic Era, specifically the Jurassic epoch. In the Permo-Triassic period, the Matruh Basin was a component of a large continental basin called the Shushan-Matruh Basin (**Avseth and Bachrac, 2005**). In the Late Jurassic-Early Cretaceous period, the process of separating northern Africa from Europe, known as Tethyan rifting, resulted in the formation of various rift basins, one of which is the Matruh Basin (**Moustafa, 2020**). The early rifting phase during the Jurassic and Early Cretaceous led to the deposition of excellent source rocks in

Matruh Basin, with TOC values up to 10%. The Late Cretaceous-Early Paleocene inversion led to the development of NNE oriented folds, dissected by NW trending normal faults, which form excellent hydrocarbon traps.

Lithostratigraphy

The sedimentary succession in the northern Western Desert, including the Matruh Basin, is divided into four primary depositional sequences (DSQ) (Fig.2). DSQ1 represents the primary regressive cycle of the Early-Middle Jurassic period, characterized by sediments of fluvial-lacustrine, deltaic, and shallow marine origin of Ras Qattara

and Khatatba formations. It was ended by a later marine transgression in the Late Jurassic, which deposited the thick carbonate section of Masjid Formation. DSQ2 corresponds to the primary regressive cycle of the Early-middle Cretaceous period, accumulating sediments from fluvio-deltaic and shallow marine environments. This cycle is represented by Alam El Bueib, Alamein, Dahab, Kharita, and Bahariya formations. DSQ3 is a significant

transgression cycle during the Late Cretaceous, characterized by the deposition of open marine shale and carbonates of Abu Roash and Khoman formations. DSQ4 is a significant transgression cycle during the Late Paleogene and Early Neogene periods, involving the deposition of open marine shales and carbonates due to Miocene regional folding and basin inversion in northern Egypt (Sultan and Halim 1988; Moustafa, 2002).

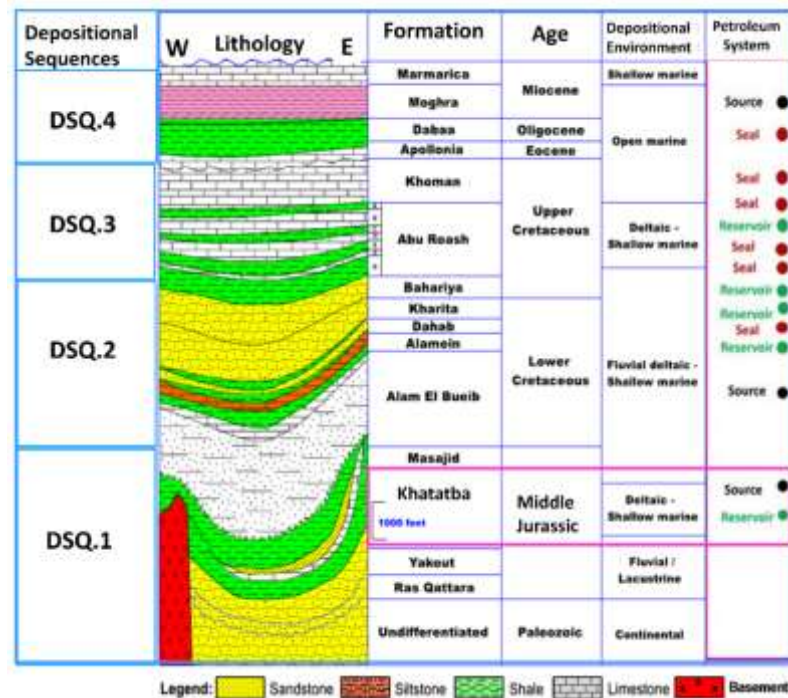


Fig. (2): Stratigraphic column of the Matruh Basin, North Western Desert, Egypt, showing 4 main depositional sequences with the lithology, age, depositional environments, and petroleum system elements of the formations Modified after Aram et al., 1988; EGPC, 1992)

Materials and Methods:

The data includes composite logs and electric well logs from Apidos-1X-well in southern Matruh Basin, and Rock Eval data for 14 cutting samples, with

measured vitrinite reflectance. The Composite log provided the depths, thicknesses, and names of the subsurface studied formations needed for the construction of the 1-D burial history

models (**Waples, 1985**). The time of deposition of each lithostratigraphic unit is also included to calculate the rate of subsidence and sedimentation throughout the basin geologic history (Table 1). The electric well logs provided the bottom hole temperature (BHT) that were used in calculating the geothermal gradient (Table 2). The BHT is corrected by the simple correction method using the time since circulation (**Waples et al., 2004**). A number of 14 shale samples in Apidose-1X-well were subjected to Rock-Eval pyrolysis analyses, where the hydrogen index (HI), total organic carbon (TOC), and kerogen type are important input parameters for calculating maturities and hydrocarbon expulsion in a 1D-Basin Model (**Fagelnour et al., 2019**). These samples were obtained from Zahra and Safa members of the Khatatba Formation. The vitrinite reflectance (R_o) was calculated from the measured maximum temperature (T_{max}) of the pyrolyzed samples calibrated with the measured vitrinite sample. Moreover, both the geothermal gradient and vitrinite reflectance were used for calibrating the burial history models and assuming the right heat flow needed for source rock maturation in the studied well (**Abd El Gawad et al., 2019**). The PetroMod-1D software was used for burial history construction and model calibration.

Boundary conditions and model calibration

The boundary conditions that are needed for constructing a 1D basin model include the sediment-water interface temperature at the top of the model and the paleo-heat flow at the bottom (**Ahmed, 2008**). The tentative paleowater depth is based on palynological and foraminiferal analysis of ditch samples for the Cretaceous age (**Abd El Kireem et al., 1996; Ahmed, 2008**). Sediment-water interface temperature depends on water depth and paleolatitude, synthesized after **Wygrala (1989)**. The basal heat flow values are specified for each geologic event using the known plate tectonic framework and crustal evolution models (**Allen and Allen, 1990, 2005**).

Basin modeling of Matruh Basin

Matruh Basin lies in the northwestern part of the Western Desert and has a NNE-SSW orientation. The basin shows an early rifting phase during the Jurassic and Early Cretaceous when Jurassic and Lower Cretaceous source rocks were deposited, with total organic carbon (TOC) up to 5% (**Moustafa, 2008**). The basin was inverted in Late Cretaceous-Late Paleocene time leading to the development of NNE oriented fault-propagation folds dissected by NW-oriented normal faults (**Bevan and**

Moustafa, 2012). These folds form excellent hydrocarbon traps as in Matruh, Apidose Field. Matruh Basin is considered as one of Early Mesozoic (Tethyan) rifting phase formed rift basins oriented NE-SW to ENE-WSW affecting mainly the northern part of Egypt due to opening of the Neotethys and divergence between the Afro-Arabian and Eurasian Plates (**Moustafa, 2020**). The modeling of Matruh Basin is

performed by building 1D-burial history models for Apidos-1X well. The 1D-burial model shows the subsidence history, sedimentation rate, maturation and time of hydrocarbon generation at the well location, and also gives profitable information about the basin history (**Waples 1985; Younes 2006; Khaled et al., 2014**).

Table (1): Tops, Bottoms, Thicknesses and Ages of the modeled subsurface units in Apidos-1X well, Matruh Basin. (AEB, BAH, AR) refer to Alam El Bueib, Baharyia, and Abu Roash formations respectively

Well Layer	Apidos-1X			Age (Ma)	
	Top ft.	Base ft.	Thick ft.	From	To
Marmarica	0	763	763	15.1	0
MOGRA	763	1891	1128	23.7	15.1
DABAA	1891	3015	1124	41.2	23.7
APOLLONIA	3015	3349	334	66	41.2
KHOMAN	3349	4357	1008	87.5	66
AR_AB	4357	4903	546	90	87.5
AR_CDE	4903	5325	421	93	90
AR_F1-G	5325	6350	1026	94	93
BAH	6350	7452	1101	100.5	94
KHARITA	7452	9000	1549	113	100.5
DAHAB	9000	9177	176	119	113
Alamein	9177	9426	249	121	119
AEB_1	9426	10064	639	123	121
AEB_3A	10064	10601	537	126	123
AEB_3E	10601	11002	401	129	126
AEB_3G	11002	11876	874	132	129
AEB_4	11876	12193	316	135	132
AEB_5	12193	12665	473	140	135
AEB_6	12665	13766	1100	145	140
MASAJID	13766	14573	808	163.5	145
ZAHRA	14573	14863	290	169	163.5
U.SAFA	14863	15548	685	170	169
Kabrit	15548	15584	36	171	170
L.SAFA	15584	16353	769	174.1	171
Ras Qattara	16353	16550	197	201.3	174.1

Table (2): Corrected bottom hole temperature (BHT) and the calculated temperature gradients

Well	BHT (°F)	Circulation time (hrs.)	Corrected BHT (°F)	T Gradient (°F/1000 ft.)
Apidos-1X	296	24	307.8	15.2

Hydrocarbon expulsion modeling of Matrouh Basin

The amount of hydrocarbon generated and expelled (oil and gas) was evaluated based on the transformation ratio (TR) and kerogen type (**Abdel Gawad et al., 2019**). The transformation ratio is defined as the ratio of the amount of generated hydrocarbons to the total amount of hydrocarbons that the kerogen is capable to generate. The transformation ratios increase with increasing maturity and were used to predict the timing of petroleum generation and expulsion (**Waples, 1985**). The transformation ratio (TR) or the production index (PI) is calculated from the following equation: $TR (PI) = S1 / (S1 + S2)$ (**Waples, 1985**) Where:

S1: free or distillable hydrocarbons which are available for migration (generated by pyrolysis of kerogen at temperature above 250°C). It is measured by milligram hydrocarbons/gm. of rock.

S2: hydrocarbons generated from kerogen upon pyrolysis, generated at maximum temperature (420- 460 °C). It

is measured by milligram hydrocarbons/gm. of rock.

Boundary conditions of Apidos-1X well

The boundary conditions of Apidos-1X well are presented in Fig. (3). The oldest paleowater depth recorded 98 ft. during the Late Triassic (212 Ma ago) in the north Western Desert sedimentary basins (Fig. 3a). The maximum paleowater depth (1986 ft.) was recorded by the end of the Cretaceous (69.1 Ma ago), while the north Western Desert was uplifted from the Paleocene and recorded zero ft. of water depth in recent times. The sediment-water interface temperature (SWIT) is estimated based on the paleowater depth and the current geographic latitude, which is 30° to the north. The SWIT (Fig. 3b) was at its maximum (84.2°F) in the Late Triassic Age (212 Ma ago) and recorded its minimum value (58.51°F) by the end of the Cretaceous Age (69.1 Ma ago). The boundary conditions of Apidos-1X well are presented in Fig. (3). The oldest paleowater depth recorded 98 ft. during

the Late Triassic (212 Ma ago) in the north Western Desert sedimentary basins (Fig. 3a). The maximum paleowater depth (1986 ft.) was recorded by the end of the Cretaceous (69.1 Ma ago), while the north Western Desert was uplifted from the Paleocene and recorded zero ft. of water depth in recent times. The sediment-water interface temperature

(SWIT) is estimated based on the paleowater depth and the current geographic latitude, which is 30° to the north. The SWIT (Fig. 3b) was at its maximum (84.2°F) in the Late Triassic Age (212 Ma ago) and recorded its minimum value (58.51°F) by the end of the Cretaceous Age (69.1 Ma ago).

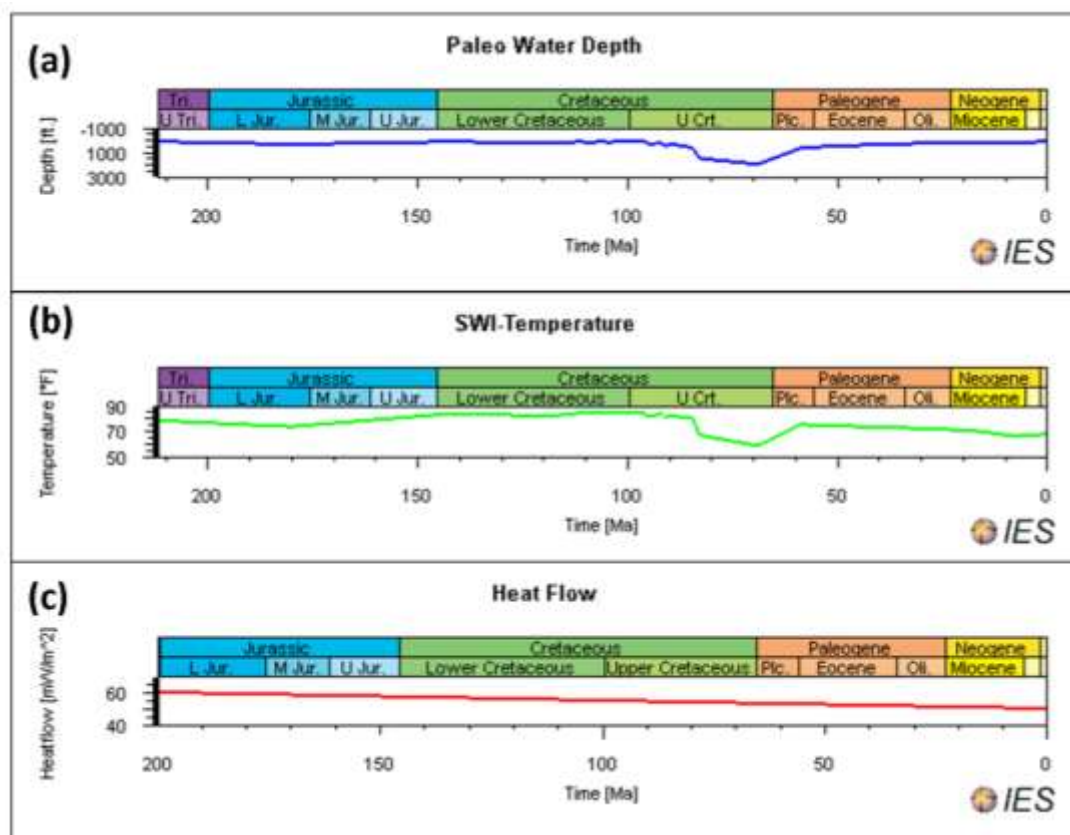


Fig. (3): The boundary conditions for Apidos-1x well: (a) Paleowater depth, (b) Sediment water interface temperature, (c) Heat flow

The average heat flow of different rift basins in the north Western Desert ranges between 50 and 70[mW/m²] according to different authors (Bosworth et al., 2015; Abd El Gawad et al., 2019; Fagelnour et al., 2019; Bosworth and Tari, 2021). The

assumed heat flow value in this study ranges between 50 and 60 [mW/m²] as shown in Fig.(3c), which is characteristic of most rift basins around the world (Allen and Allen 2005). The assumed heat flow value is calibrated by the measured vitrinite reflectance and the

calculated geothermal gradient for the modeled well (Shalaby et al., 2008; Abd El Gawad et al., 2019; Edress et al., 2021). Both the vitrinite reflectance and geothermal gradient values are coincident and show a gradual increase with depth and burial, unless the vitrinite reflectance values are modified by uplift and erosion during the geologic history (Suggate 1998). The calculated maturity and temperature gradient profiles of the Apidos-1X well are shown in Figure 4. The vitrinite reflectance (Ro) is calculated from the maximum temperature (Tmax) obtained from the pyrolysis of Zahra, Upper Safa, Kabrit, and Lower Safa samples.

Vitrinite reflectance and temperature model

Although the calculated (Ro) in Apidos-1X well (Fig. 5a) is scattered around the calculated maturity profile, the calculated temperature gradient shows a good match with the temperature gradient values measured from BHT (Fig. 5b) which indicates that the model is thermally well calibrated. Both the maturity and temperature gradient curves are gradually increasing with the increased depth of burial, and this is important for organic matter transformation into hydrocarbons through time (Galhom et al., 2022).

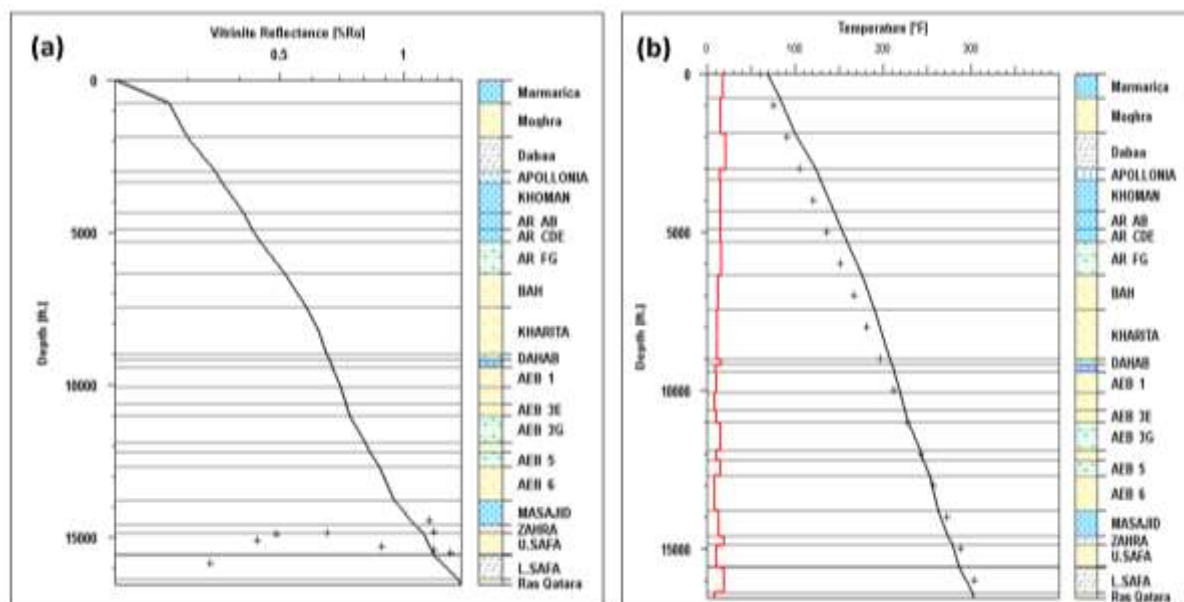


Fig. (4): (a) The calculated (solid line) and measured (+) vitrinite reflectance, and (b) the calculated and measured temperature gradient for Apidos-1X well.

Sedimentation and subsidence rate

The deposition of sediments in a basin is caused by the interplay between the pace at which the basin subsides, the amount of material flowing into it, and the height of the water column (Allen and Allen, 1990, 2005). The sedimentation rate can be determined by monitoring the accumulation of sedimentary layers during a specific time period, while accounting for erosion and non-deposition events. The geologic succession in the north Western Desert is categorized into four significant depositional cycles, with each cycle being terminated by a substantial maritime transgression (Sultan and Halim, 1988). The sedimentation rate analysis of Apidos-1X well (Fig. 5) indicates that the initial cycle began with Jurassic rifting and resulted in the accumulation of shales, sandstones, and siltstones from the Safa and Zahra members. The Upper Safa member exhibited the highest sedimentation rate, reaching approximately 300 ft./Ma. The reason for this is that during the beginning of the rift, the rate at which sediment is deposited is high, which causes the rate of subsidence to increase. At the base of the sedimentary basin, shales are the primary rocks that serve as a source for the hydrocarbon (Bosworth et al., 2015). The deposition of the Late

Jurassic Masajid Formation, consisting of transgression marine limestone, marked the end of this cycle (Keeley et al., 1990). The second cycle commenced during the Early Cretaceous period with the sedimentation of Alam El Bueib (AEB) clastic rocks. It ended with the deposition of the Alamein Formation carbonates, which occurred as a result of a high stand sea level, and was deposited, in shallow marine “inner shelf” settings. The highest reported sedimentation rate in this cycle is approximately 180 feet per million years, during which the process of rifting and subsidence persisted with a sedimentation rate lower than that during the initial stage of rift formation (Fig. 5). The third cycle began during a significant period of geological activity known as major rifting in the Late Cretaceous Time. During this time, the water depth reached its maximum level, reaching up to 1880 feet. As a result, the deep marine shales and limestones of the Abu Roash Formation were deposited. The highest sedimentation rate was seen through the deposition of Abu Roash G and F (AR F-G) members (reaching up to 580 ft./Ma) that occurred during the commencement of the rift (see Fig.5). The final sedimentary cycle took place during the Paleocene-Oligocene Time and resulted in the deposition of

limestones and shales from the Apollonia and Dabaa formations. These formations exhibit the lowest known

rates of sedimentation in the studied well, reaching up to 45 feet per million years.

Sedimentation Rate, Apidos-1X

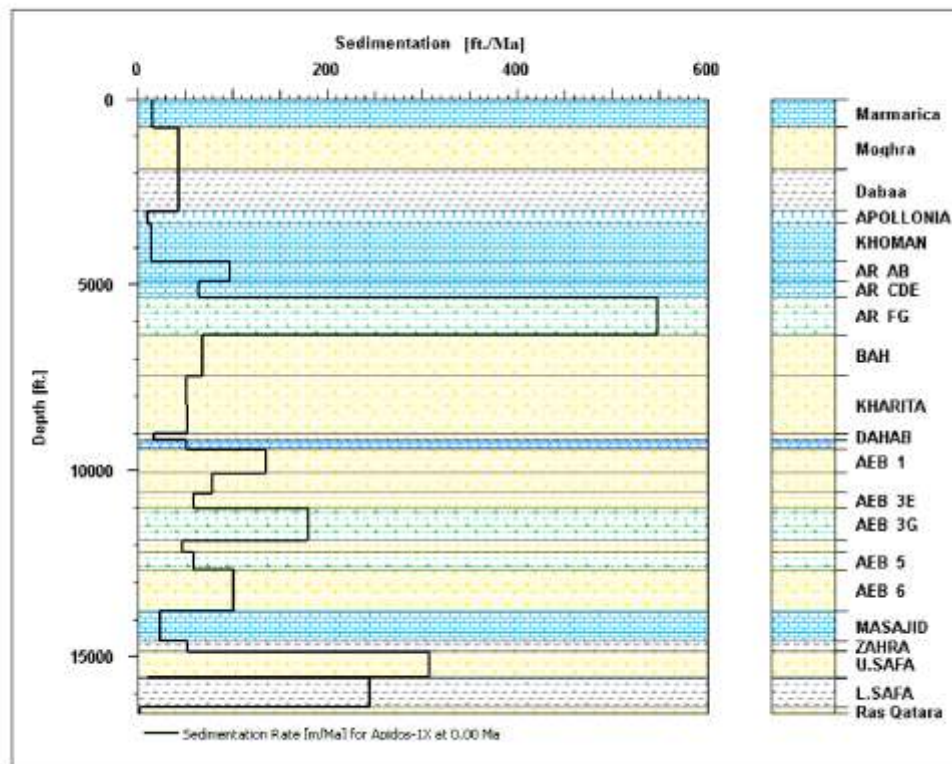


Fig.(5): The sedimentation rate of Apidos-1X well.

Burial and maturity history modeling

The burial history models of the Apidos-1X well were created using the PetroMod-1D software, which employed the **Sweeny and Burnham (1990)** easy cracking approach. The model, as shown in Figure 6, suggests the occurrence of two primary rifting stages. The first phase took place during the Middle Jurassic period approximately 173-170 million years ago, while the second phase occurred in the Late Cretaceous period around 93-92 million years ago.

During the transition from the Cretaceous to Late Paleocene Time, approximately 60-58 million years ago, there was a significant period of uplift caused by tectonic inversion. During the initial stage of tectonic subsidence caused by Jurassic rifting, the basin exhibited a fluvial, near-shore to shallow marine environment with a water depth of around 100-200 ft. Sediments such as fluvial sandstones, siltstones, and shallow marine shales and limestones were deposited in this setting. The presence of shale source rocks in the

Zahra and Lower Safa members, as well as sandstone reservoir rocks in the Upper Safa Member, is clearly indicated in Fig. (6). The process of subsidence persisted throughout the Early Cretaceous period. This was marked by the accumulation of fluvial sediments in the Alam EL Bueib Formation, namely during the Early Cretaceous time. These sediments were intercalated by alternating layers of shallow marine shales and carbonate deposition, forming repeating cycles (Fagelnour et al., 2018). Subsequently, the carbonates of the Aptian Alamein Formation are deposited, along with the marine shales and siltstones of the Dahab Formation, and the river sandstones of the Kharita Formation (EGPC 1992; Schlumberger 1995).

The end of the Early Cretaceous period was marked by a moderate uplift and erosion in the stratigraphic section and the formation of the Cenomanian Baharyia Formation during the Late Cretaceous. This formation consisted of clay-rich sandstones and siltstones that were produced in a coastal to shallow marine environment (Abd El Fattah et al., 2018). In the Late Cretaceous period, there was a significant increase in the subsidence and accumulation of sediment in a deep marine environment, with water depths ranging from around 1500 to 1880 feet (Fig. 6). This resulted in the formation of deep marine limestones and shales known as the Abu Roash Formation.

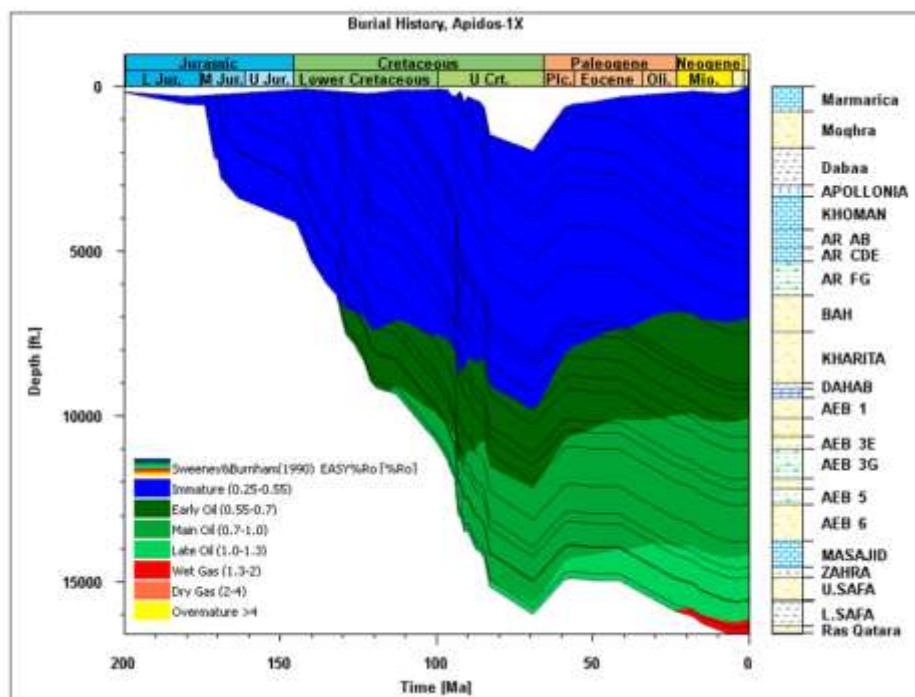


Fig. (6): The burial history of Apidos-1X well.

The end of the Cretaceous-Early Paleocene was characterized by regional unconformity in the north Western Desert of Egypt due to uplift and erosion, followed by the deposition of limestones from the Apollonia Formation, shales from the Dabaa Formation, and sandstones from the Moghra Formation. The whole cycle ended with the deposition of the great limestone plateau of the Marmarica Formation, which covers most of the north Western Desert of Egypt (**Sultan and Halim 1988; Said 1990**). These phases of tectonic subsidence and inversion are responsible for the deposition of the main reservoir and source rocks and the formation of structural traps that originated during the Mesozoic period in the Matruh Basin. As a result of deposition, burial, and increasing pressure and temperature with the depth of the source rocks, organic matter (OM) is transformed into oil and/or gas (**Tissot and Welte 1984; Hunt 1995**).

Expulsion modeling

Expulsion is modeled to start at a transformation ratio (TR) of 10%. Expelled early oil, peak oil, and late oil windows are defined at TRs ranging from 10 to 25%, 25 to 50%, and 50 to 80%, respectively. More than 80%

include the beginning of cracking oil to gas, with the cracking to gas ending with a TR of 99% (**Hantschel et al., 2009; Hakimi et al., 2018**). Kerogen type, total organic carbon (TOC%), and hydrogen index (HI) for the studied Zahra and Lower Safa shale source rocks are listed in Table 3. The hydrocarbon generation and expulsion histories based on the calculated TR and modeled Ro of the source rocks in the studied well, Apidos-1X, is shown in Table 4 and Fig. (7). For Zahra member source rock shale, the first stage of hydrocarbon generation of Zahra shale in the Apidos-1x well occurred during the Late Cretaceous at 93–90 my. This stage is the early phase of oil generation without any expulsion. The TR of Zahra shale varied from 10 to 25% during this stage, with a computed Vitrinite reflectance (Ro) of 0.68–0.73%. The second stage (90–86 my) at Late Cretaceous is the main phase of the oil generation with TR 25 to 50% and calculated Ro 0.73–0.78. The third stage is the late oil stage, with TR 50 to 80% and Ro 0.78 to 0.85 at Late Cretaceous to Paleocene (86 to 56 my). The fourth stage is the cracking of oil to gas with TR from 80 to 100% and Ro from 0.85 to 1.09 % in Paleocene to Recent time (56-0 my) (Table 4 and Fig. 7).

Table (3): Kerogen type, total organic carbon (TOC %), and hydrogen index (HI) for the studied Zahra and Lower Safa shale source rocks in Apidos-1X well

Well	Unit	Kerogen type	HI (mg HC/ g TOC)	TOC %
Apidos-1X	Zahra	III	165	10
	Lower Safa	III	145	3

Table (4): The calculated TR and modeled Ro of the source rocks in Apidos-1X well.

Well	Fm/ Unit	Onset oil generation				Main oil generation			
		TR %	Ro %	Time (Ma)	Age	TR %	Ro %	Time (Ma)	Age
Apidos-1X	Zahra	10-25	0.68-0.73	93-90	Late Cretaceous	25-50	0.73-0.78	90-86	Late Cretaceous
	L.Safa	10-25	0.67-0.73	112-98	Early- Late Cretaceous	25-50	0.73-0.78	98-92	Late Cretaceous
	Fm/ Unit	Late oil generation				Cracking oi to gas			
		TR %	Ro %	Time (Ma)	Age	TR %	Ro %	Time (Ma)	Age
	Zahra	50-80	0.78-0.85	86-56	Late Cretaceous-Paleocene	80-100	0.85-1.09	56-0	Paleocene-Recent
L.Safa	50-80	0.78-0.88	92-87	Late Cretaceous	80-100	0.88-1.27	87-0	Late Cretaceous-Recent	

For the Lower Safa member, the first stage of hydrocarbon generation of Lower Safa shale in Apidos-1x well occurred during the Early to Late Cretaceous at 112–98 my. This stage is the early phase of oil generation without any expulsion. The TR of Lower Safa shale varied from 10 to 25% during this stage, with a computed Vitrinite reflectance (Ro) of 0.67–0.73%. The second stage (98–92 my) at Late Cretaceous is the main phase of the oil generation with TR 25 to 50%

and calculated Ro 0.73–0.78. The third stage is the late oil stage, with TR 50 to 80% and Ro 0.78 to 0.88 at Late Cretaceous (92 to 87 my). The fourth stage is the cracking of oil to gas with TR from 80 to 100% and Ro from 0.88 to 1.27 % in Late Cretaceous to Recent time (87–0 m) (Table 4 and Fig. 7).

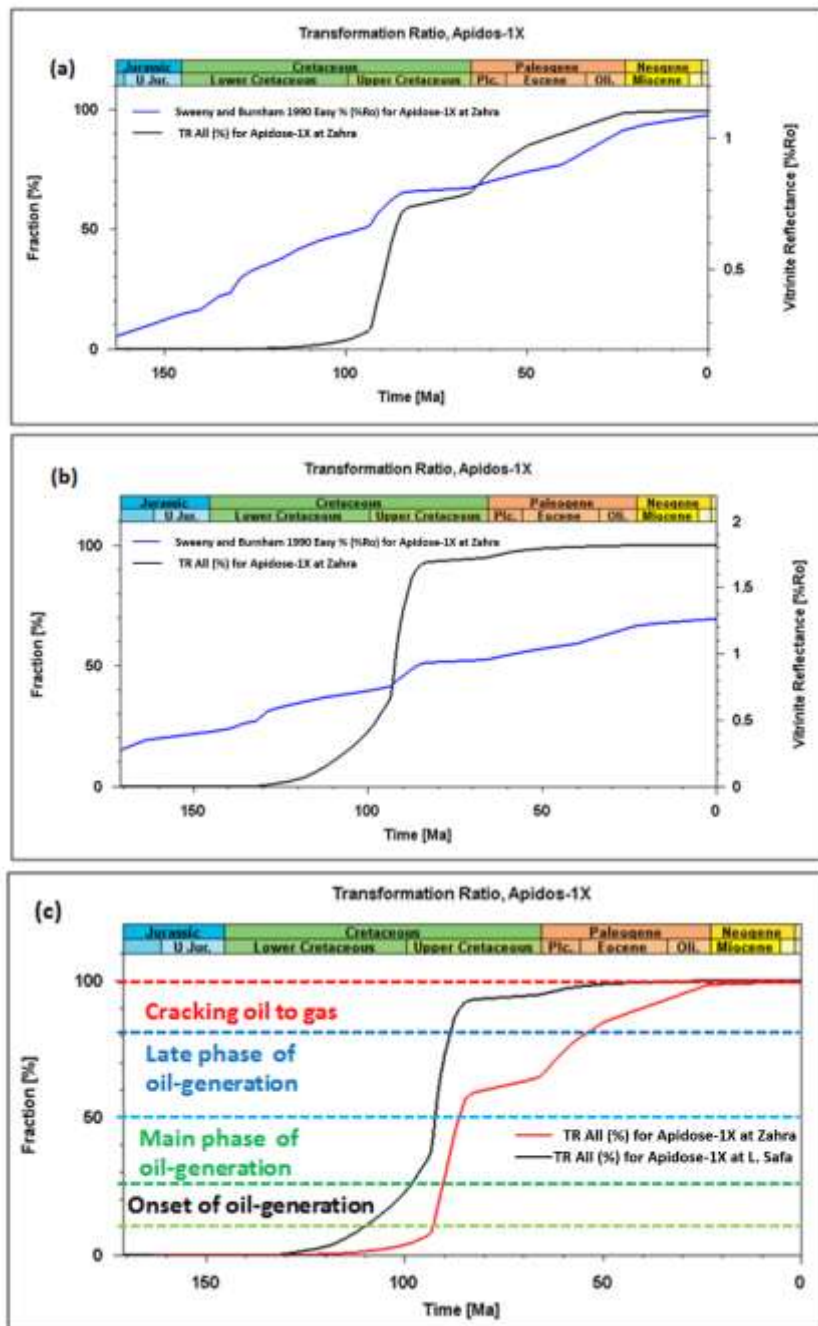


Fig. (7): (a) Transformation ratio and vitrinite reflectance versus time, Zahra Shales, (b) Transformation ratio and vitrinite reflectance versus time, Lower Safa Shales, (c) Evolution of the transformation ratio with age, Apidos-1X well.

Based on the previously constructed burial history models in (Fig.5) the onset and depth of main oil generation (R_o 0.7-1) and wet gas generation (R_o 1.3-2) are summarized in Table 5. The onset of oil generation occurred in the Early Cretaceous time (115-116 Ma

ago), while the onset of gas generation happened in the Oligocene time (22-24 Ma ago). On the other hand, the depth of main oil window is located on depth 9650 to 10050 ft., and that of wet gas window is located at depth from 15550 to 16000 ft.

Table (5): The onset and depth of main oil generation (Ro% 0.7-1) and wet gas generation (Ro% 1.3-2).

Well	Onset of oil generation (Ma)	Onset of Gas Generation (Ma)	Depth of main oil window (ft.)	Depth of wet gas window (ft.)
Apidos-1X	115	22	10050	16000

Petroleum system of Matruh Basin

The petroleum system includes all elements of petroleum generation and accumulation in a basin (Walters, 2006). These elements include source rocks, reservoir rocks, and seal rocks, geological structures forming petroleum traps, and faults that act as conduits for hydrocarbons' migration (Peters and Cassa, 1994). The petroleum system events chart for the Apidos-1X well is shown in (Fig. 8). The well includes the elements of the petroleum system in the Matruh Basin,

and the timing of these elements is important for the entrapment of generated hydrocarbons. The shale source rocks were deposited in the Middle Jurassic (175–163 Ma ago) and include Zahra and Lower Safa members. The sandstone reservoir rocks of the Ras Qattara Formation, Upper Safa, and AEB-6 members have been deposited in the Early and Middle Jurassic and Early Cretaceous, respectively (200–140 Ma ago) (Bosworth et al., 2015).

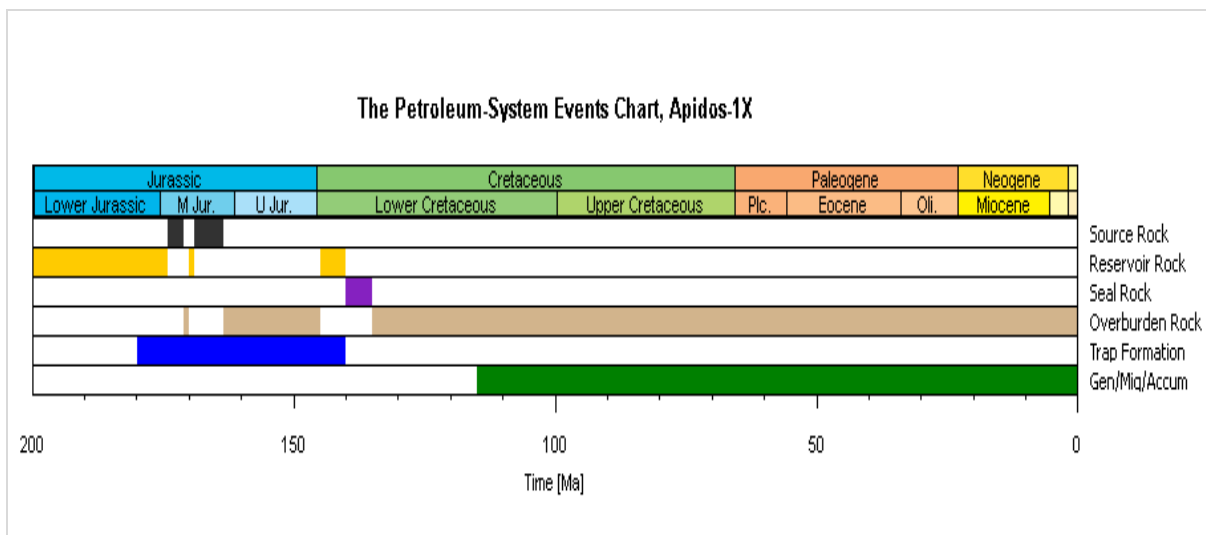


Fig. (8): The petroleum system events chart of Apidos-1X well

Shales and siltstones of the AEB-5 Member act as the main seal rock and were deposited in the Early Cretaceous (140–135 Ma ago). The main structural traps formed in the Jurassic–Early Cretaceous period (180–140 Ma ago), and the onset of oil generation, migration, and accumulation started in the Early Cretaceous period (116–115 Ma ago) (Moustafa 2008, 2020). The traps formed during the Jurassic and Cretaceous rifting phases of the Matruh Basin were later charged by petroleum through migration and accumulation, which is characteristic of all Mesozoic rift basins in the north Western Desert of Egypt (Taha 1992).

Summary and conclusion

Available geological and geochemical data from the Apidos-1X well have been used to construct 1-D burial history models in order to study tectonic events, petroleum generation, and entrapment in the Matruh Basin. The assumed heat flow value in this study ranges between 50 and 60 [mW/m²], which is characteristic of most rift basins around the world. The calculated (Ro%) shows a good match with the calculated maturity curve, and the calculated temperature gradient coincides with that measured from BHT, where the models are thermally well calibrated. The sedimentation rate

models of the well show four major depositional cycles, each of which ends with a marine transgression. Two maximum sedimentation rates occurred: one in the first cycle (Jurassic rifting) and the other in the third cycle (Early Cretaceous rifting). The maximum sedimentation occurred during rift initiation, where source rocks were accumulated at the base (i.e., Zahra, Lower Safa, and AR-F1-G members). The constructed burial history models showed that the onset of oil generation occurred in the Early Cretaceous period (115–116 Ma ago), while the onset of gas generation happened in the Oligocene period (22–24 Ma ago). On the other hand, the depth of the main oil window is located at 9650 to 10050 ft., and that of the wet gas window is located at 15550 to 16000 ft. The Matruh Basin includes all the elements of the petroleum system, where the shale source rocks were deposited in the Middle Jurassic (175–163 Ma ago) and include Zahra and Lower Safa members. The sandstone reservoir rocks of the Ras Qattara Formation, Upper Safa, and AEB-6 members have been deposited in the Early and Middle Jurassic and Early Cretaceous, respectively (200–140 Ma ago). The shales and siltstones of the AEB-5 Member act as the main seal rock and

were deposited in the Early Cretaceous (140–135 Ma ago). The main structural traps formed in the Jurassic–Early Cretaceous period (180–140 Ma ago), and the onset of oil generation, migration, and accumulation started in the Early Cretaceous period (116–115 Ma ago). Hydrocarbon later charged the traps created during the Matruh Basin's Jurassic and Cretaceous rifting phases through migration and accumulation.

Acknowledgements

Authors are very grateful for the Egyptian General Petroleum Corporation (EGPC) and Khalda Petroleum Company for permission and granting rock samples and well logging data of the Apidos-1X well.

References

- Abdel-Fattah, M. I., Metwalli, F. I., & El Sayed, I. M. (2018).** Static reservoir modeling of the Bahariya reservoirs for the oilfields development in South Umbarka area, Western Desert, Egypt. *J. Afri. Ear. Sci.*, 138, 1-13.
- Abd El Gawad, E. A., Ghanem, M. F., Lotfy, M. M., Mousa, D. A., Temraz, M. G., & Shehata, A. M. (2019).** Burial and thermal history simulation of the subsurface Paleozoic source rocks in Faghur basin, north Western Desert, Egypt: Implication for hydrocarbon generation and expulsion history. *Egypt. J. Petrol.*, 28(3), 261-271.
- Abdel-Kireem, M. R., Schrank, E., Samir, A. M., & Ibrahim, M. I. A. (1996).** Cretaceous palaeoecology, palaeogeography and palaeoclimatology of the northern Western Desert, Egypt. *J. of Afri. Ear. Sci.*, 22(1), 93-112.
- Ahmed, M. A. A. (2008).** Geodynamic evolution and petroleum system of Abu Gharadig basin, north western desert, Egypt (Doctoral dissertation, Aachen, Techn. Hochsch., Diss., 2008).
- Allen, A.P., and Allen, R.J. (1990).** Basin analysis: principles and applications (First ed.). 451 pp. Oxford, Blackwell Scientific Publications.
- Allen, A.P., and Allen, R.J. (2005).** Basin analysis: principles and applications (Second ed.). 549 pp. Oxford, Blackwell Scientific Publications, 'Original', Basin analysis: Principles and Applications.
- Aram, R. B., Roehl, N. L., & Feazel, C. T. (1988).** Seismic stratigraphy and subsurface geology of the north-central portion of the South Umbarka Concession, Western Desert, Egypt. Phillips Petroleum Company report, 11.
- Avseth, P., & Bachrac, R. (2005).** Seismic properties of unconsolidated sands: Tangential stiffness, V_p/V_s ratios and diagenesis. In SEG International Exposition and Annual Meeting (pp. SEG-2005). SEG.
- Bevan T.G., Moustafa A.R. (2012).** Inverted rift-basins of northern Egypt. In: Phanerozoic Rift Systems and Sedimentary Basins. Elsevier, pp. 483-507.
- Bosworth W., Drummond M., Abrams M., Thompson M. (2015).** Jurassic rift initiation source rock in the Western Desert, Egypt – relevance to exploration in other continental rift systems, in: Petroleum Systems in “Rift” Basins, 34th Annual GCSSEPM Foundation Perkins Rosen Research Conference, 13–16 December 2015, Houston.
- Bosworth W, Tari G (2021)** Hydrocarbon accumulation in basins with multiple phases of extension

- and inversion: examples from the Western Desert (Egypt) and the western Black Sea. *Solid Earth*, 12: 59-77, 2021.
- Dolson, J. C., Shann, M. V., Matbouly, S. I., Hammouda, H., & Rashed, R. M. (2001).** Egypt in the twenty-first century: petroleum potential in offshore trends. *GeoArabia*, 6(2): 211-230.
- Edress NAA, Darwish S, Ismail A (2021)** Geochemical characterization of the source rock intervals, Beni-Suef Basin, West Nile Valley, Egypt. *Open Geosciences*, 13(1): 1536-1551.
- EGPC Egyptian General Petroleum Corporation (1992)** Western Desert, oil and gas fields. In: EGPC 11th Petroleum Exploration and Production Conference, Cairo, Egypt (a comprehensive overview): Al-Ahram Commercial Presses, Cairo, 431 p. EOG, 2023. <https://egyptoilgas.com/publications/february-2023/>
- Fagelnour M.S., Metwalli F.I., Shendi E.H. (2018)** Structural and facies modeling of the Lower Cretaceous Alam El Bueib reservoirs in the Shushan Basin, Western Desert, Egypt. *Arab. J. Geosci.* 11(9): 1-24.
- Fagelnour M.S., Gamil I., El Toukhy M., Gharieb A., Saad H. (2019)** Source Rock Potentiality, Basin Modeling, and Oil to Source Correlation in Northern Shushan Basin, Western Desert, Egypt. OMC-2019.
- Galhom, T., Mann, P., & Rudolph, K. (2022).** Jurassic-recent stratigraphy, structure, and hydrocarbon potential of the Mesozoic-Cenozoic rifted-passive margin of the Tarfaya-Dakhla basin of southern Morocco. *Marine and Petroleum Geology*, 139, 105626.
- Hakimi, M. H., Mohialdeen, I. M., Al Ahmed, A. A., & El Nady, M. M. (2018).** Thermal modeling and hydrocarbon generation of the Late Jurassic-Early Cretaceous Chia Gara Formation in Iraqi Kurdistan region, northern Zagros Fold Belt. *Egy. J. of petrol.*, 27(4): 701-713.
- Hantschel, T., & Kauerauf, A. I. (2009).** Fundamentals of basin and petroleum systems modeling. Springer Science & Business Media.
- Hunt, J. M. (1995).** Petroleum geochemistry and geology (textbook). *Petroleum Geochemistry and Geology (Textbook)*. (2nd Ed.), WH Freeman Company.
- Keeley M.L., Dungworth G., Floyd C.S., Forbes GA, King C, Garva RM, Shaw D (1990)** The Jurassic System in Northern Egypt: I. Regional stratigraphy and implications for hydrocarbon prospectivity: *J. Petrol. Geol.*, 13: 397-420.
- Khaled K.A., Attia G.M., Metwalli F.I. and Fagelnour M.S. (2014).** Subsurface Geology and Petroleum System in the Eastern Offshore Area, Nile Delta, Egypt. *J. Appl. Sci. Res.*, (4): 254-270.
- Mansour, A., Gentzis, T., Tahoun, S. S., Ahmed, M. S., Gier, S., Carvajal-Ortiz, H., & Wang, J. (2023).** Near equatorial paleoclimatic evolution and control on organic matter accumulation during the Cenomanian in the Abu Gharadig Basin, southern Tethys: Insights from palynology, organic petrography, and geochemistry. *Int. J. Coal Geol.*, 270, 104221.
- Meshref, W. M. (1999).** Cretaceous tectonics and its impact on oil exploration in northern Egypt. *Geol. Soci. of Egy. Special Publication (2)*, 199244.

- Metwalli, Farouk I., and John D. Pigott.** Analysis of petroleum system criticals of the Matruh–Shushan Basin, Western Desert, Egi.. *Petrol. Geosci.* 11.2, 157-178 (2005).
- Moustafa, A. R. (2002).** Controls on the geometry of transfer zones in the Suez rift and northwest Red Sea: Implications for the structural geometry of rift systems. *AAPG Bulletin*, 86(6), 979-1002.
- Moustafa A.R. (2008)** Mesozoic-Cenozoic Basin Evolution in the Northern Western Desert of Egypt”, 3rd Sympos. on the Sedimentary Basins of Libya (The Geology of East Libya), 3: 29-46.
- Moustafa A.R. (2020).** Mesozoic-Cenozoic Deformation History of Egypt. In: Hamimi Z., El-Barkooky A., Martínez Frías J., Fritz H., Abd El-Rahman Y. (eds) *The Geology of Egypt. Regional Geology Reviews.* Springer, Cham.
- Peters K.E., Cassa M.R. (1994).** Applied source rock geochemistry. In: Magoonand, L. B., Dow, W. G., (Eds.) *The petroleum system from source to trap.* AAPG Bulletin, 93-120.
- Said R. (1990)** *The Geology of Egypt.* Balkema-Rotterdam-Brookfield.
- Schlumberger (1995)** Well evaluation conference, Egypt. EGPC Report.
- Shalaby R. M, Abdullah W. H., Shady A. N (2008)** “ Burial history, basin modeling and petroleum source potential in the Western Desert, Egypt”. *Bulletin of the Geol. Soci. of Malaysia* 54 (2008): 103 – 113.
- Shalaby M.R., Hakimi M.H., Abdullah W.H. (2014).** Petroleum system analysis of the Khatatba Formation in the shoushan basin, north Western Desert, Egypt. *Arabian J. Geosci.* 7, 4303–4320.
- Suggate P.R. (1998)** Relations between depth of burial, vitrinite reflectance and geothermal gradient. *J. of Petrol. Geol.*, 21(1): 5-32.
- Sultan N., Halim M.A. (1988)** Tectonic Framework of northern Western Desert, Egypt & its effect on hydrocarbon accumulations. *Proc.9th E.G.P.C. Petrol. Expl. and Prod. Conf.,*2: 1-22.
- Sweeney J.J., Burnham AK (1990)** Evaluation of a simple model of vitrinite reflectance based on chemical kinetics. *AAPG Bulletin*, 74: 1559-1570.
- Taha M.A (1992)** Mesozoic rift basins in Egypt: their southern extension and impact on future exploration. *Proceedings of the 11th Petrol. Expl. and Prod. Conf., Cairo, 1988. EGPC,* 2: 1-19.
- Tissot B.P., Welte D.H. (1984)** *Petroleum Formation and Occurrence.* 2nd ed. Heidelberg: Springer- Verlag, 699 p.
- Walters C. (2006)** The origin of petroleum In: *Practical Advances in Petroleum Processing.*
- Waples D.W. (1985).** *Geochemistry in petroleum exploration.* Int. Human Res. and Dev. Corp., Boston, 226 p.
- Waples D.W., Pacheco J., Vera A. (2004).** A method for correcting log-derived temperatures in deep wells, calibrated in the Gulf of Mexico. *Petroleum Geoscience*, 10(3): 239-245.
- Wygrala, B.P. (1989).** Integrated study of an oil field in the southern Po basin, northern Italy. Unpublished Dissertation thesis, Berichte Kernforschungsanlage Jülich, University of Köln, Köln. 217 pp.

Younes, M. A. (2006). Petroleum system in the shushan basin: a mature basin leading to future exploration in the western desert of Egypt. In Adapted

from extended abstract for oral presentation at AAPG Annual Convention, Houston, Texas.

محاكاة تاريخ الدفن والنضج الحراري لصخور المصدر الجوراسي الأوسط بحوض مطروح شمال الصحراء الغربية، مصر

د. ولاء عواد على* ، د. محمد فحج النور**

*قسم جيولوجيا البترول، كلية علوم البترول والتعدين، جامعة مطروح، مطروح، ٥١٥١١، مصر

** شركة خالدة للبترول، القاهرة، مصر

يتناول البحث نمذجة تكوين الخطاطبة (الجوراسي الأوسط)، والذي يُعتبر صخور المصدر للهيدروكربونات في حوض مطروح بالصحراء الغربية في مصر، باستخدام البيانات الجيولوجية والجيوكيميائية من بئر (أبيدوس-X1). تم إنشاء نموذج تاريخ الدفن لبيتر بواسطة برنامج PetroMod-1D باستخدام طريقة التكسير البسيطة التي استخدمها سويني وبورنهام عام (١٩٩٠). وتساعد النمذجة الأحادية الأبعاد للحوض في استنتاج تواريخ الدفن والحرارة، والتنبؤ بتوقيت تخليق النفط وانتقاله من صخور المصدر إلى صخور الخزان البترولي. وقد حدد النموذج مرحلتين للتصدع، واحدة في العصر الجوراسي الأوسط (قبل ١٧٣-١٧٠ مليون سنة مضت) والأخرى في أواخر العصر الطباشيري (قبل ٩٣-٩٢ سنة مضت)، مع أعلى معدلين للترسيب. تميزت نهاية العصر الطباشيري إلى العصر الباليوسيني المبكر (منذ ٦٠ إلى ٥٨ مليون سنة مضت) بمرحلة رفع كبيرة للمكونات الجيولوجية بسبب الانقلاب التكتوني. وتشير النماذج المبنية إلى أن متكون الخطاطبة دخل بداية تكوين النفط في العصر الطباشيري المبكر (قبل ١١٥-١١٦ مليون سنة مضت)، في حين أن بداية توليد الغاز حدثت في فترة الأوليغوسين (قبل ٢٢-٢٤ مليون سنة مضت). ولوحظ انه حدث تكسير النفط إلى غاز في الصخور المصدرية للعصر الجوراسي الأوسط في بئر (أبيدوس-X1).

يشتمل حوض مطروح على جميع عناصر النظام البترولي، مع صخور مصدر الصخر الزيتي من العصر الجوراسي الأوسط، وصخور الحجر الرملي (الخزان البترولي) من العصر الجوراسي المبكر والأوسط، وصخور الغطاء الصخري (الغير نفاذة) من العصر الطباشيري المبكر. بدأ توليد النفط وهجرته وتراكمه في أوائل العصر الطباشيري، حيث كانت الهيدروكربونات تهاجر للمصيدة البترولية من خلال الفوالق التي حدثت في بداية مراحل التصدع. تشير نتائج نمذجة حوض مطروح في موقع البئر ابيدوس 1X إلى أن صخور المصدر الجوراسي الأوسط تعمل كصخور مصدر فعالة، حيث من المتوقع أن يتم توليد كمية كبيرة من البترول واطلاقها إلى صخور الخزان المحتملة القريبة في حوض مطروح.